Retinoblastoma (Rb) regulates laminar dendritic arbor reorganization in retinal horizontal neurons

Rodrigo A. P. Martins[a,b,1], Denise Davis[a,1], Ryan Kerekes[c], Jiakun Zhang[a], Ildar T. Bayazitov[a], Daniel Hiler[a], Mahmut Karakaya[d], Sharon Frase[e], Shaun Gleason[c], Stanislav S. Zakharenko[a], Dianna A. Johnson[f], and Michael A. Dyer[a,f,g,2]

[a]Department of Developmental Neurobiology, St. Jude Children's Research Hospital, Memphis, TN 38105; [b]Instituto de Biofísica Carlos Chagas Filho, Centro de Ciências da Saúde, Universidade Federal do Rio de Janeiro, 21941-900, Rio de Janeiro, Brazil; [c]Measurement Science and Systems Engineering Division, Oak Ridge National Laboratory, Oak Ridge, TN 37831; [d]Department of Electrical Engineering and Computer Science, University of Tennessee, Knoxville, TN 37996; [e]Cell and Tissue Imaging, St. Jude Children's Research Hospital, Memphis, TN 38105; [f]Department of Ophthalmology, University of Tennessee Health Science Center, Memphis, TN 38163; and [g]Howard Hughes Medical Institute, Chevy Chase, MD 20815

Edited* by Constance L. Cepko, Harvard Medical School/Howard Hughes Medical Institute, Boston, MA, and approved November 8, 2011 (received for review June 6, 2011)

Neuronal differentiation with respect to the acquisition of synaptic competence needs to be regulated precisely during neurogenesis to ensure proper formation of circuits at the right place and time in development. This regulation is particularly important for synaptic triads among photoreceptors, horizontal cells (HCs), and bipolar cells in the retina, because HCs are among the first cell types produced during development, and bipolar cells are among the last. HCs undergo a dramatic transition from vertically oriented neurites that form columnar arbors to overlapping laminar dendritic arbors with differentiation. However, how this process is regulated and coordinated with differentiation of photoreceptors and bipolar cells remains unknown. Previous studies have suggested that the retinoblastoma (*Rb*) tumor suppressor gene may play a role in horizontal cell differentiation and synaptogenesis. By combining genetic mosaic analysis of individual synaptic triads with neuroanatomic analyses and multiphoton live imaging of developing HCs, we found that Rb plays a cell-autonomous role in the reorganization of horizontal cell neurites as they differentiate. Aberrant vertical processes in *Rb*-deficient HCs form ectopic synapses with rods in the outer nuclear layer but lack bipolar dendrites. Although previous reports indicate that photoreceptor abnormalities can trigger formation of ectopic synapses, our studies now demonstrate that defects in a postsynaptic partner contribute to the formation of ectopic photoreceptor synapses in the mammalian retina.

retina | synaptogenesis

Neuronal differentiation and synaptogenesis must be coordinated precisely during development to ensure that appropriate neural circuits are formed and maintained through an organism's lifetime. In vertebrate retinas, defects in photoreceptor differentiation or function can affect the formation of stable synaptic triads. For example, New Zealand obese 2 (*nob2*) mice have a mutation in calcium channel, voltage-dependent, L type, alpha 1F subunit (*Cacna1f*) (1) encoding an L-type voltage-dependent calcium channel that regulates calcium entry into photoreceptor synaptic triads. *nob2* mice have ectopic synapses in the outer nuclear layer (ONL), which share features with normal synaptic triads (2). Ectopic synapses are not present during early postnatal development, suggesting that rod photoreceptors retract their terminals in *nob2*-mutant retinas, leading to outgrowth of second-order processes to maintain synaptic contact. Other mutant mouse strains with defective photoreceptor development or synaptic transmission also form ectopic synapses in the ONL (3–6). However, there are no reports of defects in postsynaptic triad elements (horizontal and bipolar cells) that lead to ectopic synapses in the ONL of mouse retinas (7–10). Synaptogenesis defects in photoreceptors, horizontal cells (HCs), and bipolar cells are important to study, because similar changes occur in many human retinopathies and their corresponding animal models (11–15).

In this study, we characterized the role of retinoblastoma (Rb) in HC development and synaptogenesis (16). Rb, originally identified as a tumor suppressor, is now known to regulate several cellular processes essential for normal development. Shortly after they are generated, newly postmitotic cells at the retinal apical surface that are committed to the HC fate migrate to their final position just below the future outer plexiform layer (OPL). During this migration, cells extend apical and basal processes that eventually are retracted and replaced by overlapping lateral projections along the OPL when cells arrive at their final position. The vertical processes drive the formation of the regular mosaic of HCs in the mature retina before lamination (17). We found that Rb is required cell autonomously for proper timing of HC maturation and synaptogenesis. Our study provides a valuable model to study the coordinated reorganization of apical processes of HCs during lamination and the initiation of synaptic triad formation.

Results

Association of Apical HC Processes and Ectopic Synapses with *Rb*-Deficient Cells in Mouse Retinas. The *Chx10-Cre* transgene is expressed in a mosaic pattern in retinal progenitor cells throughout development and in a subset of differentiated bipolar cells and Müller glia (16, 18). We reported apical HC processes and ectopic photoreceptor synapses in the ONL in *Chx10-Cre;*$Rb^{Lox/Lox}$ retinas but did not determine if the defect is autonomous to the horizontal neurons (16). To mark cells that underwent *Cre*-mediated recombination with YFP indelibly and to determine if apical HC processes are associated with *Rb*-deficient regions of retinas, we generated *Chx10-Cre;*$Rb^{Lox/Lox}$*;Rosa-YFP* mice. Apical–basal columns of cells were YFP^+ in mice at postnatal days (P) P0, P7, P14, and P21 and in adult mice (Fig. 1 *A*–*C*). All seven classes of cell types were identified within YFP^+ columns by morphology, laminar position, and coimmunolocalization studies. Horizontal sections through the inner nuclear layer (INL) showed an irregular mosaic pattern (Fig. 1 *D* and *E*). A 3D reconstruction (Fig. 1*C*) and cell scoring for 25 fields from three separate P21 animals revealed that labeled cell columns were 14.3 ± 9.1 μm in diameter at the INL.

To determine if ectopic HC processes and ectopic synapses are associated with regions of *Rb* inactivation, we studied cell-specific immunostaining patterns localized within synaptic triads or

Author contributions: R.A.P.M., I.T.B., S.G., D.A.J., and M.A.D. designed research; R.A.P.M., D.D., R.K., J.Z., I.T.B., D.H., M.K., S.F., S.G., D.A.J., and M.A.D. performed research; R.K., S.G., S.S.Z., D.A.J., and M.A.D. contributed new reagents/analytic tools; R.A.P.M., D.D., R.K., S.F., S.G., D.A.J., and M.A.D. analyzed data; and R.A.P.M., R.K., D.A.J., and M.A.D. wrote the paper.

The authors declare no conflict of interest.

*This Direct Submission article had a prearranged editor.

Freely available online through the PNAS open access option.

[1]R.A.P.M. and D.D. contributed equally to this work.

[2]To whom correspondence should be addressed. E-mail: michael.dyer@stjude.org.

This article contains supporting information online at www.pnas.org/lookup/suppl/doi:10.1073/pnas.1108141108/-/DCSupplemental.

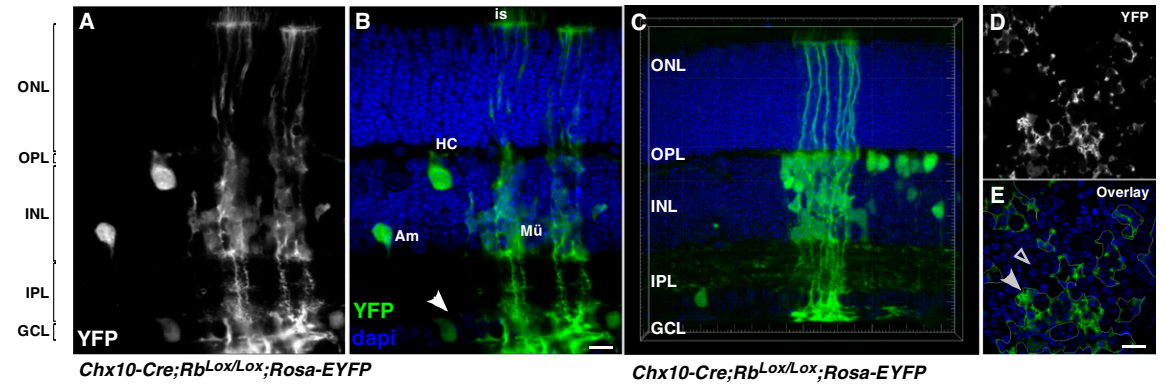

Fig. 1. YFP expression marks *Rb*-deficient cellular mosaic in *Chx10-Cre;Rb$^{lox/lox}$;Rosa-YFP* mouse retinas. (*A*) Confocal image of YFP expression in a column of cells in *Chx10-Cre;Rb$^{lox/lox}$;Rosa-YFP* P18 mouse retinas. (*B*) Overlay of YFP expression (green) with nuclear staining with DAPI (blue) to highlight the retinal laminar structure. Individual cell types are indicated, including a cell in the ganglion cell layer (arrowhead). (*C*) 3D *z*-series through another column of cells that underwent Cre-mediated recombination of *Rb^{Lox}* and the *Rosa-EYFP* reporter gene. (*D* and *E*) Confocal image of a horizontal section through the retina shown in *A* and *B* at the apical portion level of the INL, highlighting the mosaic pattern of the *Chx10-Cre* transgene activity. Arrowhead indicates mosaic patch of Rb-deficient cells, and the open arrowhead indicates a patch of normal retina. Am, amacrine cell; GCL, ganglion cell layer; HC, horizontal cell; INL, inner nuclear layer; IPL, inner plexiform layer; is, inner segments of photoreceptors; Mü, Müller glia; ONL, outer nuclear layer; OPL, outer plexiform layer. (Scale bars: 10 μm.)

processes of HC, bipolar, and photoreceptor cells. Immunostaining was visualized in the context of the genetic mosaic by coimmunolocalization with YFP in *Chx10-Cre;Rb$^{Lox/Lox}$;Rosa-YFP* and *Chx10-Cre;Rb$^{Lox/+}$;Rosa-YFP* retinas at P11–P14 and P18–P21. Of the 100 apical calbindin-immunopositive processes scored that extended at least 10 μm into the ONL (six independent retinas at both developmental stages), 97 ± 1.4% (P11–P14) and 95 ± 2.1% (P18–P21) were associated with the *Rb*-deficient mosaic (Fig. 2 *A* and *B*). Control retinas had no ectopic HC processes. To distinguish between axons and dendrites, we performed coimmunolocalization with antibodies that recognize axonal neurofilaments and calbindin (*SI Appendix*, Fig. S1). Of the 177 calbindin-immunopositive ectopic HC processes from seven independent retinas analyzed at P14 and P21, the majority (92%; 164/177) were axons.

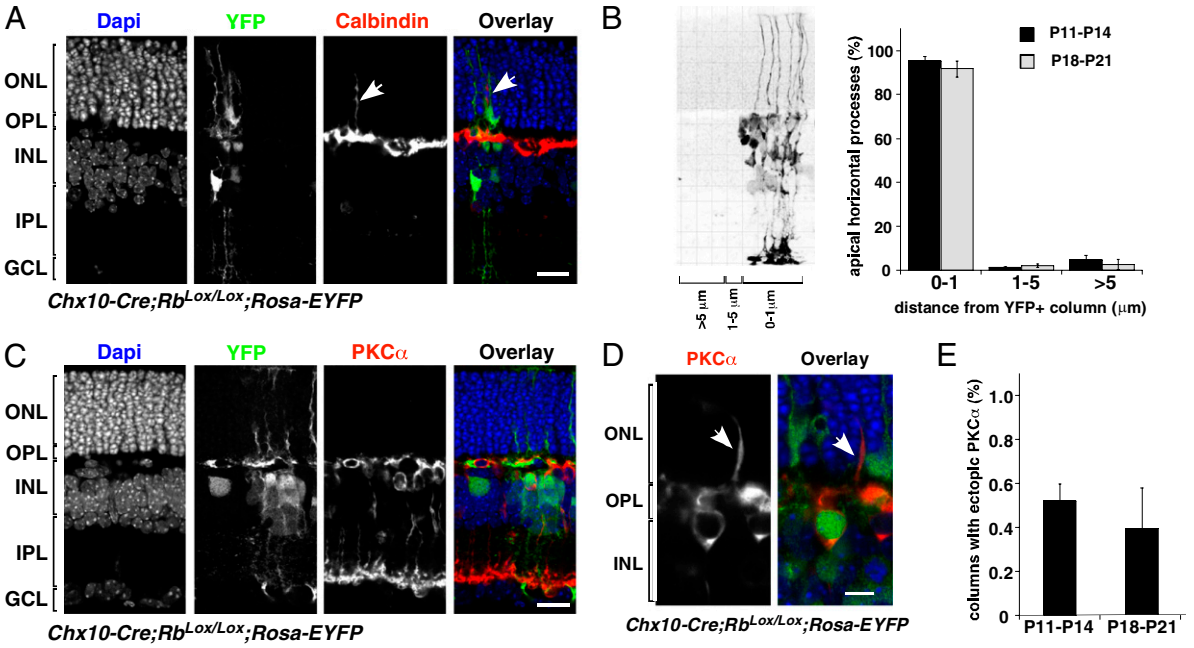

Fig. 2. HC processes do not reorganize into their laminar position in *Chx10-Cre;Rb$^{Lox/Lox}$;Rosa-YFP* mouse retinas. (*A*) Coimmunolocalization of YFP (green) and calbindin (red) in P21 *Chx10-Cre;Rb$^{Lox/Lox}$;Rosa-YFP* mouse retinas. Apical processes (arrows) of calbindin-immunopositive HCs are associated with regions of *Rb* inactivation (green). (*B*) Association of apical processes was scored with respect to distance from a column of *Rb*-deficient cells, as indicated by YFP expression. Once the apical horizontal cell process was identified, the distance from the nearest YFP$^+$ column of cells was measured, and processes were divided into a 0–1μm group (within the column of cells or touching the column on the edge); a 1–5 μm group (within approximately one cell body of the column); and a >5 μm group (beyond approximately one cell body of column). The histogram gives mean (± SD) of scoring from the six independent retinas at each stage. (*C*) PKCα-immunopositive rod bipolar cells did not extend dendrites into the ONL in *Rb*-inactivated (green) or wild-type regions at P21. (*D*) A rare ectopic PKCα dendrite in *Chx10-Cre;Rb$^{Lox/Lox}$;Rosa-YFP* retinas (arrow) adjacent to a patch of YFP-expressing cells (green). (*E*) Histogram showing mean (± SD) scoring from the six independent retinas at each stage. Bip, bipolar cell; GCL, ganglion cell layer; HC, horizontal cell; INL, inner nuclear layer; IPL, inner plexiform layer; ONL, outer nuclear layer; OPL, outer plexiform layer. (Scale bars: 10 μm.)

To determine if PKCα-immunopositive bipolar cells extended dendrites into the ONL, we examined 250 YFP^+ columns of cells (six independent retinas at P11–P14 and P18–P21) and scored the number of ectopic PKCα-immunopositive processes. Ectopic bipolar cell processes were very rare and did not extend beyond 10 μm into the ONL (Fig. 2 *C–E*); if present, ectopic PKCα-immunopositive processes were not associated with ectopic HC processes. To extend our analysis to cone bipolar cells, we performed coimmunolocalization with anti–calcium-binding protein 5 (Cabp5) and anti-GFP antibodies (19, 20). We could find no evidence of ectopic cone bipolar dendrites in *Chx10-Cre;*$Rb^{Lox/Lox}$*;Rosa-YFP* mice (*SI Appendix*, Fig. S2). To validate these data independently, we generated *Chx10-Cre;*$Rb^{Lox/Lox}$*;mGluR6-GFP* mice that express GFP in both rod and cone bipolar cells (21). There was no evidence for the type of ectopic bipolar processes reported previously in retinas, in which terminals are believed to retract into the ONL (*SI Appendix*, Fig. S2).

Next, we characterized the colocalization of the synaptic ribbon protein bassoon with YFP in *Chx10-Cre;*$Rb^{Lox/Lox}$*;Rosa-YFP* and *Chx10-Cre;*$Rb^{Lox/+}$*;Rosa-YFP* retinas at P11–P14 and P18–P21. We visualized 100 YFP^+ columns (six independent retinas at P11–P14 and P18–P21) and scored the number of ectopic bassoon punctae within the YFP^+ region (*SI Appendix*, Fig. S3 *A* and *B*). We also scored 100 adjacent YFP^- regions. Ectopic synapses were abundant, with ∼33% of YFP^+ columns containing ectopic bassoon punctae (*SI Appendix*, Fig. S3*C*) at each stage. Columns containing ectopic bassoon immunofluorescence in the ONL had 3–21 individual punctae (*SI Appendix*, Fig. S3*D*). Analysis of postsynaptic density protein 95 (PSD95), another synaptic protein localized to photoreceptor terminals (22), gave similar results (*SI Appendix*, Fig. S3 *E–H*). Coimmunolocalization of calbindin and bassoon showed association of ectopic bassoon punctae with terminals of ectopic HC processes in the ONL (*SI Appendix*, Fig. S3 *I–K*).

Genetic Mosaic Analysis of Normal and Ectopic Synaptic Triads in Mouse Retinas. To characterize the structure of ectopic synapses and to determine if Rb has a cell-intrinsic role in this process, we generated *Chx10-Cre;*$Rb^{Lox/Lox}$*;Z/AP* mice, in which all retinal cells that undergo Cre-mediated recombination are marked indelibly with human placental alkaline phosphatase (ALPP). A modified lead citrate-staining procedure was used to visualize ALPP expression on membranes of individual neurons and processes in electron micrographs (16, 18). Therefore, this mouse strain is ideal for genetic mosaic analysis at the individual-synapse level (*SI Appendix*, Figs. S4 and S5). Electron micrographs showed that the mosaic pattern of Cre-mediated recombination was similar to that of YFP expression from *Chx10-Cre;*$Rb^{Lox/Lox}$*;Rosa-YFP* mice (*SI Appendix*, Fig. S4). The number of labeled bipolar cell bodies (21/56; 37%) and synaptic triads with labeled dendrites (81/224; 36%) was consistent with mosaic expression of the *Chx10-Cre* transgene (*SI Appendix*, Fig. S4).

To determine if Rb-deficient HCs and bipolar cells form normal synaptic connections, 41 OPL spherules at or near areas of ALPP-labeled cells were analyzed for the presence of labeled HC or bipolar processes in the synaptic triad. In 68% of triads (28/41), labeled bipolar dendrites and/or HC processes were identified, indicating their origin from ALPP-expressing *Rb*-deficient bipolar cells or HCs.

Ectopic synapses were identified in *Cre;*$Rb^{Lox/Lox}$*;Z/AP* retinas, and ALPP-labeled elements were present in ectopic synapses (*SI Appendix*, Fig. S5). Scoring of 28 individual ectopic synapses for the presence of labeled HC processes showed that all ectopic synapses contained ALPP-labeled (*Rb*-deficient) horizontal processes. In one ectopic synapse <10 μm apical from the OPL, labeled elements in the synapse had no synaptic vesicles, suggesting it was a bipolar dendrite. This observation is consistent with the rare ectopic short bipolar dendrites identified in *Chx10-Cre;*$Rb^{Lox/Lox}$*; Rosa-YFP* retinas.

Serial sectioning and 3D reconstruction of individual synaptic triads at the OPL and the ectopic location in the ONL were used to determine if *Rb*-deficient HCs form invaginating synapses with photoreceptor terminals in their ectopic location (Fig. 3). These studies confirmed that ectopic synapses are invaginating synapses (Fig. 3 *B* and *D*) and, as shown in coimmunolocalization analyses, do not contain bipolar dendrites.

Automated Scoring of *Rb*-Deficient HC Morphology During Development. The Gad-67-GFP transgenic mouse line expresses GFP in developing HCs (17). Our electron microscopic genetic mosaic analysis demonstrated that virtually all apical HC processes that form stable ectopic synapses are derived from *Rb*-deficient cells. Therefore, we can monitor the development of *Rb*-deficient HCs that contribute to ectopic synapses by characterizing the morphology of cells with persistent apical processes. To do so, we generated *Chx10-Cre;*$Rb^{Lox/Lox}$*;GAD67-GFP* mice. Multiple fields were analyzed by multiphoton confocal microscopy spanning central-to-peripheral positions at P4, P5, P6, P7, P8, and P12. The stage between P4 and P7 is critical, because HC processes undergo columnar-to-lateral laminar orientation during this period (17). This dramatic transition can be visualized in 3D reconstruction of confocal images of GFP expression in control and *Rb* conditional knockout retinas (Fig. 4 *A–H*). Apical processes emanating from the *Rb*-deficient HC can be identified in this developmental time course (Fig. 4 *A–H*).

To quantify the morphologic features of *Rb*-deficient HCs accurately and to compare them with wild-type cells, we developed an automated segmentation, skeletonization, and tracing algorithm (Fig. 4 *I* and *J*) (23) and tested it by comparison with semimanual tracing using Imaris software for 275 cells at multiple developmental stages with tracings from the algorithm. These data agreed well for both datasets and allowed the scoring of hundreds of cells across each stage. In the 1,181 HCs analyzed (data are available upon request), there was no significant difference in the

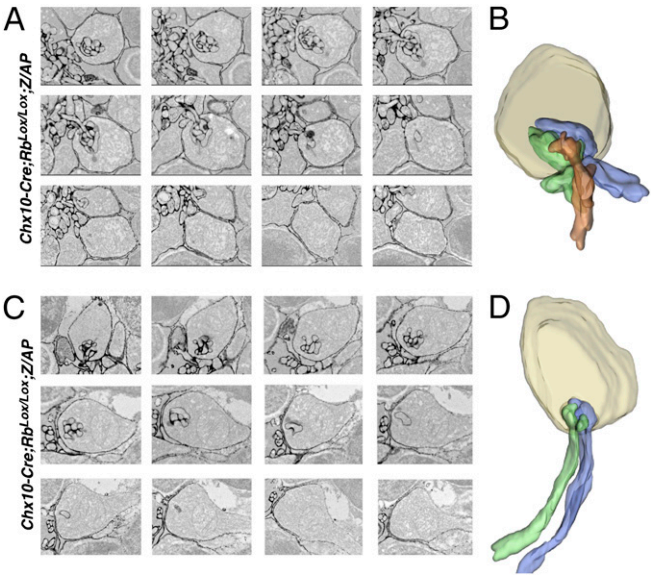

Fig. 3. Serial sectioning and 3D reconstruction of ectopic and normal synaptic triads. (*A*) Electron micrographs of serial sections from the outer plexiform layer showing labeled bipolar and horizontal elements in a synaptic triad. (*B*) 3D reconstruction of micrographs in *A* with individual horizontal neurites shown in green and blue and the bipolar dendrite shown in orange. (*C*) Electron micrographs of serial sections from the ONL showing labeled horizontal elements in an ectopic synaptic triad. (*D*) 3D reconstruction of the micrographs in *C* with individual horizontal neurites shown in green and blue. No bipolar dendrites were observed.

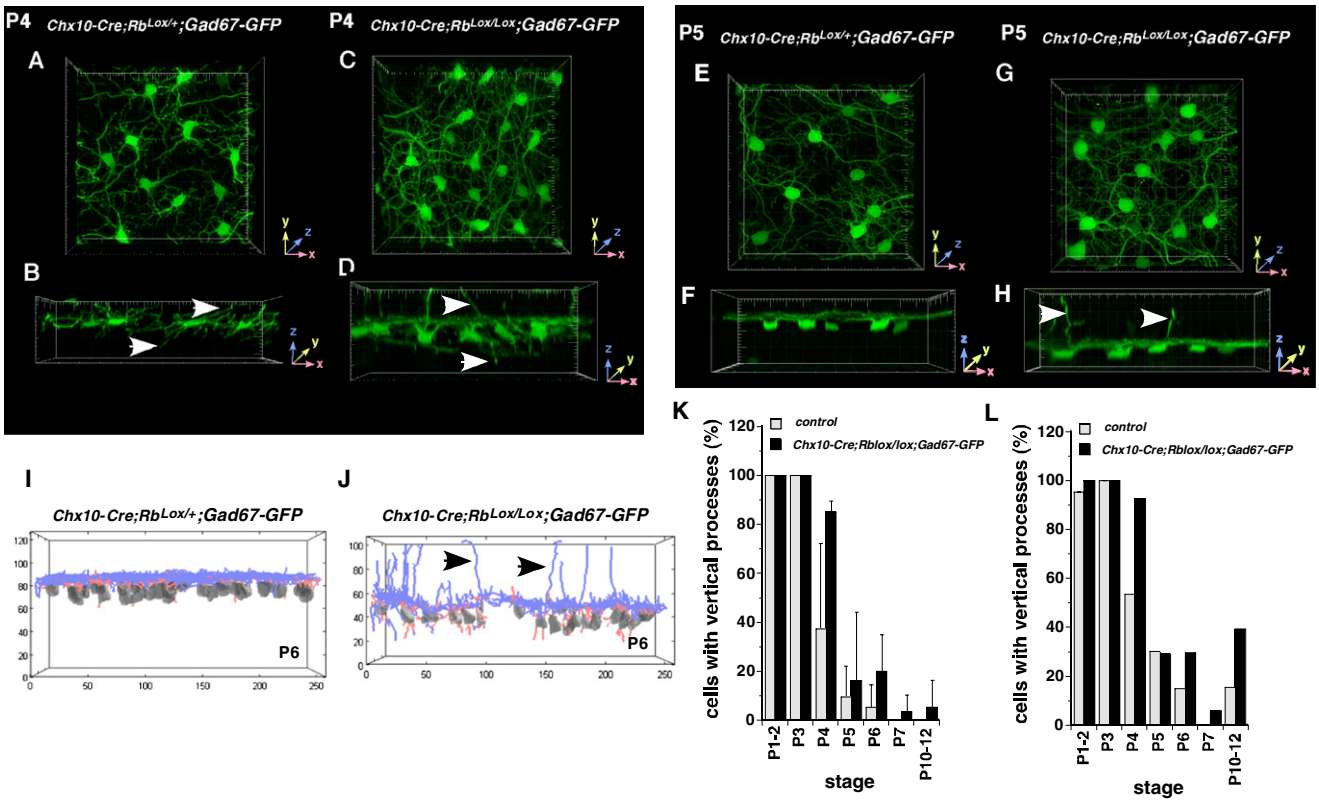

Fig. 4. Reorganization of horizontal cell processes during development. (*A–D*) 3D multiphoton confocal images of representative fields of control (*A* and *B*) and *Rb*-deficient (*C* and *D*) retinas showing GFP-labeled HCs at P4. Top view is shown in *A* and *C*, and the corresponding side view is shown in *B* and *D*. Arrows indicate apical and basal processes. Individual grid marks correspond to 1-μm increments. (*E–H*) 3D multiphoton confocal images of representative fields of control (*E* and *F*) and *Rb*-deficient (*G* and *H*) retinas showing GFP-labeled HCs at P5. The top view is shown in *E* and *G*, and the corresponding side view is shown in *F* and *H*. Arrows indicate apical processes still present in the absence of Rb. Individual grid marks correspond to 1-μm increments. (*I* and *J*) 3D reconstructions and automated tracings of a representative field of GAD67-GFP expression in HCs in control (*I*) and *Rb*-deficient (*J*) retinas. Arrows indicate apical processes still present in the absence of Rb. (*K* and *L*) Histograms showing proportion of cells with vertical processes at each developmental stage. Each bar represents the mean (± SD) of multiple independent retinas and multiple fields of view within each retina. Data plotted in *K* correspond to the semi-manual tracing results, and those in *L* correspond to automated tracing.

overall developmental timing of the morphologic transition from vertical to lateral cell processes in *Chx10-Cre;Rb$^{Lox/+}$;GAD67-GFP* and *Chx10-Cre;Rb$^{Lox/Lox}$;GAD67-GFP* retinas (Fig. 4 *K* and *L*).

To determine if *Rb*-deficient HCs with apical processes resemble immature cells from an earlier development stage or are a hybrid of mature and less-differentiated cells, the algorithm was used for a detailed morphometric analysis of HCs with apical processes in *Chx10-Cre;Rb$^{Lox/Lox}$;GAD67-GFP* retinas (*SI Appendix*, Figs. S6 and S7), and these data were compared with data from the developmental time course. At P7 or later (P10–P12), the branching and angles of ectopic processes in *Cre;Rb$^{Lox/Lox}$;GAD67-GFP* HCs were similar to those of immature wild-type HCs at earlier stages (P3, P6), but processes were approximately half the length of those in wild-type HCs (*SI Appendix*, Fig. S6).

Live Imaging of HCs. Analysis of the developmental time course of *Chx10-Cre;Rb$^{Lox/Lox}$;Gad67-GFP* retinas suggests that apical HCs from *Rb*-deficient cells fail to reorganize laterally during development, because these processes remain vertically arranged at all developmental stages. In contrast, in other mutant mouse models in which photoreceptor terminals retract or new processes extend into the ONL forming ectopic synapses, there is a period when normal columnar–lateral reorganization has occurred and there are no ectopic processes. However, if the period of photoreceptor terminal retraction/new process formation overlaps with normal columnar–lateral reorganization, the persistence of apical processes of HCs that do not reorganize cannot be distinguished from photoreceptor terminal retraction/HC sprouting.

These two possibilities were distinguished by multiphoton live imaging of *Chx10-Cre;Rb$^{Lox/Lox}$;Gad67-GFP* retinas for 18–24 h at P6–P7 to visualize individual HCs during this critical transition. Data from three representative experiments (60 individual HCs) generated by the algorithm are presented. One series (Fig. 5 *A* and *B*) shows several apical processes that persisted throughout the time course, even as other processes associated with that cell and the processes of neighboring cells underwent columnar–lateral reorganization. This HC is a typical cell, having the apical type of HC process characterized throughout the study. In the same field, more dynamic changes occurred near the cell body, consistent with retraction/sprouting of new processes (*SI Appendix*, Fig. S8); these processes did not extend beyond 10 μm apical to the OPL. Many HCs also matured normally, showing stable processes in the imaging time series (*SI Appendix*, Fig. S8). The length and dynamics of processes over the time course allowed us to classify and quantify each process for all cells in the three experiments (Fig. 5 *C* and *D*). Taken together these data suggest that most, if not all, of the long HC apical processes that form ectopic synapses in the mature retina persist from earlier in development and reflect a defect in laminar reorganization of HC processes in the absence of Rb.

Discussion

Here, we show that Rb contributes cell autonomously to HCs in the critical process of reorganizing their neurites to the laminar

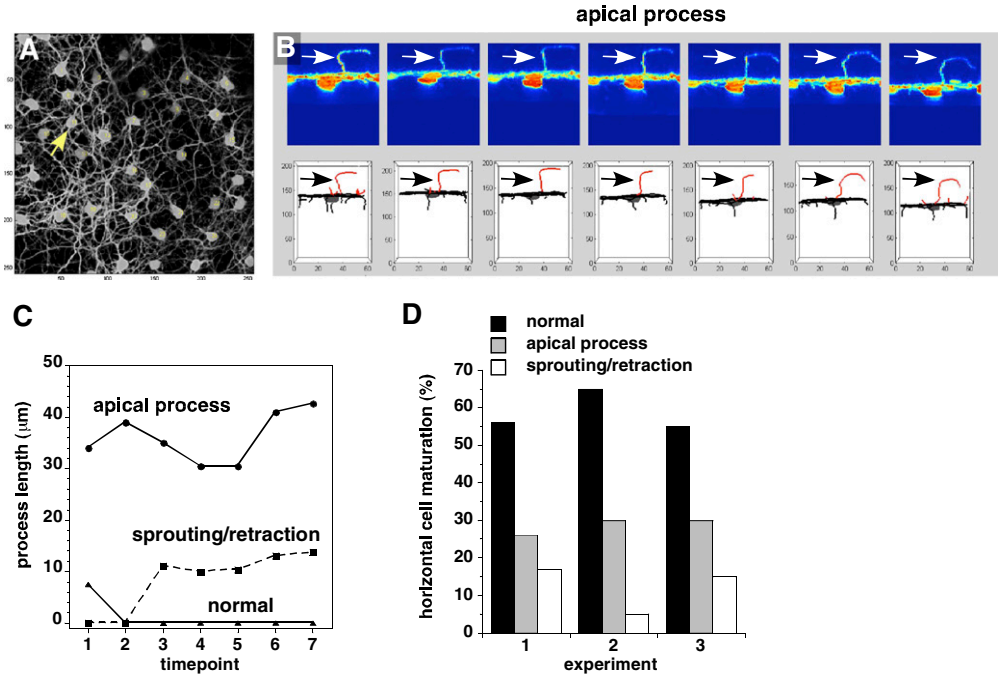

Fig. 5. Multiphoton live imaging of HCs in *Chx10-Cre;Rb*$^{Lox/Lox}$*;Gad67-GFP* retinas. (*A*) Top view of a representative field with 20 HCs. Arrow indicates cells shown in *B*. (*B*) Side view (*Upper*) of a single cell with a persistent apical process (arrow) and the corresponding 3D tracing of that cell (*Lower*) at seven representative sequential 1-h time points. Apical processes are shown in red. Arrows indicate an ectopic HC process. (*C*) The length of the processes was plotted to represent a persistent apical process (*Top*), a process that showed dynamic changes during the time course (sprouting/retraction) (*Center*), and a process that underwent normal maturation (*Bottom*). (*D*) Histogram of the proportion of cells in three experiments with persistent apical processes, dynamic changes in their processes (retraction/sprouting), and normal processes.

position. In the absence of Rb, persistent apical processes form ectopic invaginating synapses with photoreceptors within the ONL. Coimmunolocalization studies demonstrated that the great majority of ectopic processes are axons, and this observation is consistent with the presence of ectopic rod terminals (24, 25). The ectopic synapses are stable in adult retinas and do not receive synaptic input from bipolar dendrites. These results and conclusions are based on the unique application of transmission electron microscopy (TEM)-based genetic mosaic analysis in the developing mammalian CNA at the level of individual synaptic elements. Approximately 33% of mosaic columns of YFP$^+$ cells had ectopic HC synapses, a percentage that is slightly higher than the percentage of columns with YFP$^+$ HC bodies. Therefore, we propose that most Rb-deficient HCs have defects in reorganizing some processes during development.

Developmental and multiphoton live imaging studies suggest that ectopic processes and synapses do not result from photoreceptor terminal retraction or neurite sprouting from HCs, and this notion is supported by the absence of bipolar dendrites in ectopic synapses. In studies of genetically engineered mouse models or retinal degeneration models, apical processes often result from the retraction of the photoreceptor terminal caused by a defect in photoreceptors themselves. In contrast, our results show that persistent columnar processes and ectopic synapses result from a cell-autonomous defect in a cell that forms postsynaptic contacts in the photoreceptor triad. Notably, the absence of Rb in developing HCs does not affect other steps in HC differentiation such as migration and synaptogenesis at the OPL. Future studies on molecular targets of Rb in developing HCs may help elucidate the pathways that regulate this key process during retinal neurogenesis.

Rb, first associated with retinoblastoma, has been implicated in many cellular processes related to tumorigenesis and normal development. Because *Rb* is proposed to be a key regulator of transcriptional programs that facilitate the transition from immature proliferating cells to their terminally differentiated progeny, it has been implicated in cellular differentiation in various tissues and organs.

HCs rely on homotypic interactions among apical processes during early development and migration to establish a regular mosaic; on reaching their laminar position, processes reorganize into overlapping laminar arbors (17). We found that these apical processes are close to photoreceptor terminals as they extend through the ONL toward the OPL. However, synaptogenesis usually is not initiated in the ONL; there is a delay until HCs are reorganized and photoreceptor terminals reach the presumptive OPL. One explanation for this coordination is that HC processes are not competent to form synapses when they extend apically in the ONL early in development but do so only after reorganizing to the lateral configuration; that is, both the timing and location of terminals/processes is key for synaptogenesis.

We propose a model to explain the role of Rb in HC maturation. In the absence of Rb, apical horizontal processes can acquire the competence to form synapses with photoreceptor terminals in their apical orientation extending into the ONL. If so, then when an Rb-deficient HC process encounters a developing photoreceptor terminal, it initiates synaptogenesis ectopically in the ONL and is retained in the adult retina. According to this model, some processes from Rb-deficient HCs may form normal synaptic triads at the OPL because they reorganize into the lateral position before they encounter a photoreceptor terminal in the ONL. Single-cell gene-expression studies of Rb-deficient and wild-type HCs may shed light on the transcriptional network that controls HC synaptic competence.

Materials and Methods

Mice. *Chx10-Cre;Rb*$^{Lox/Lox}$ mice have been described previously (26). *Z/AP* and *RosaYFP* mice were obtained from Jackson Labs, and *GAD-67-GFP* mice (27) have been described previously (17). The mGluR6-GFP also mice have been

described previously (21). The St. Jude Animal Care and Use Committee approved all animal studies.

Coimmunolocalization and Confocal Microscopy. Retinas were isolated in PBS and fixed for 1 h in 4% (wt/vol) paraformaldehyde. Whole retinas were embedded in 4% (wt/vol) agarose in PBS and cut into 50-μm sections on a vibratome. Sections were blocked in 5% (vol/vol) normal goat serum, 0.5% (vol/vol) Triton X-100 in PBS for 1 h at room temperature, and incubated in primary antibody in the same block solution for 1 h (*SI Appendix, SI Materials and Methods*). Images were acquired with a Zeiss LSM700 confocal microscope.

TEM and Lead Citrate Staining. TEM and lead citrate staining were performed as described previously (16). Details are given in *SI Appendix, SI Materials and Methods*.

Multiphoton Live Imaging Studies. Whole-retina flat mounts were cultured for 18–24 h at 35 °C in oxygenated Ames medium (pH 7.4) containing 20 mM Hepes, 40 mM glucose, 100 U/mL penicillin G, and 100 μg/mL streptomycin; the perfusion rate was 1 mL/min. Two-photon laser-scanning microscopy was performed using an Ultima imaging system (Prairie Technologies) with a Ti: sapphire Chameleon Ultra femtosecond-pulsed laser (920 nm) (Coherent). Images were acquired with a 40× 0.8 NA water-immersion IR objective (Olympus). Eight-bit images of 512 × 512 pixels (0.223 μm per pixel in the *x–y* axis) with 0.5-μm *z*-steps were acquired with a 20× 0.8 NA water-immersion IR objective (Olympus). Images were analyzed by Imaris software (Bitplane) or our automated algorithm.

ACKNOWLEDGMENTS. We thank Marina Kedrov for assistance with image processing and scoring and Vani Shanker for editing the manuscript. This work was supported in part by Cancer Center Support Grant CA21765 from the National Cancer Institute; by Grants EY014867 and EY018599 from the National Institutes of Health (to M.A.D.); by Fogarty International Research Collaboration Award/National Institutes of Health 1R03TW008344-01 (to M.A.D. and R.A.P.M.); by the American Cancer Society; by the Research to Prevent Blindness Foundation; and by the American Lebanese Syrian Associated Charities. M.A.D. is a Howard Hughes Medical Institute Early Career Scientist.

1. Chang B, et al. (2006) The nob2 mouse, a null mutation in Cacna1f: Anatomical and functional abnormalities in the outer retina and their consequences on ganglion cell visual responses. *Vis Neurosci* 23:11–24.
2. Bayley PR, Morgans CW (2007) Rod bipolar cells and horizontal cells form displaced synaptic contacts with rods in the outer nuclear layer of the nob2 retina. *J Comp Neurol* 500:286–298.
3. Ball SL, et al. (2002) Role of the beta(2) subunit of voltage-dependent calcium channels in the retinal outer plexiform layer. *Invest Ophthalmol Vis Sci* 43:1595–1603.
4. Haeseleer F, et al. (2004) Essential role of Ca2+-binding protein 4, a Cav1.4 channel regulator, in photoreceptor synaptic function. *Nat Neurosci* 7:1079–1087.
5. Dick O, et al. (2003) The presynaptic active zone protein bassoon is essential for photoreceptor ribbon synapse formation in the retina. *Neuron* 37:775–786.
6. Haverkamp S, et al. (2006) Synaptic plasticity in CNGA3(-/-) mice: Cone bipolar cells react on the missing cone input and form ectopic synapses with rods. *J Neurosci* 26: 5248–5255.
7. Ball SL, Pardue MT, McCall MA, Gregg RG, Peachey NS (2003) Immunohistochemical analysis of the outer plexiform layer in the *nob* mouse shows no abnormalities. *Vis Neurosci* 20:267–272.
8. Gregg RG, et al. (2003) Identification of the gene and the mutation responsible for the mouse *nob* phenotype. *Invest Ophthalmol Vis Sci* 44:378–384.
9. Tagawa Y, Sawai H, Ueda Y, Tauchi M, Nakanishi S (1999) Immunohistological studies of metabotropic glutamate receptor subtype 6-deficient mice show no abnormality of retinal cell organization and ganglion cell maturation. *J Neurosci* 19:2568–2579.
10. Dhingra A, et al. (2000) The light response of ON bipolar neurons requires G[alpha]o. *J Neurosci* 20:9053–9058.
11. Fisher SK, Lewis GP, Linberg KA, Verardo MR (2005) Cellular remodeling in mammalian retina: Results from studies of experimental retinal detachment. *Prog Retin Eye Res* 24:395–431.
12. Peng YW, Hao Y, Petters RM, Wong F (2000) Ectopic synaptogenesis in the mammalian retina caused by rod photoreceptor-specific mutations. *Nat Neurosci* 3: 1121–1127.
13. Peng YW, Senda T, Hao Y, Matsuno K, Wong F (2003) Ectopic synaptogenesis during retinal degeneration in the Royal College of Surgeons rat. *Neuroscience* 119:813–820.
14. Fariss RN, Li ZY, Milam AH (2000) Abnormalities in rod photoreceptors, amacrine cells, and horizontal cells in human retinas with retinitis pigmentosa. *Am J Ophthalmol* 129:215–223.
15. Jones BW, et al. (2003) Retinal remodeling triggered by photoreceptor degenerations. *J Comp Neurol* 464:1–16.
16. Johnson DA, Donovan SL, Dyer MA (2006) Mosaic deletion of Rb arrests rod differentiation and stimulates ectopic synaptogenesis in the mouse retina. *J Comp Neurol* 498:112–128.
17. Huckfeldt RM, et al. (2009) Transient neurites of retinal horizontal cells exhibit columnar tiling via homotypic interactions. *Nat Neurosci* 12:35–43.
18. Rowan S, Cepko CL (2004) Genetic analysis of the homeodomain transcription factor Chx10 in the retina using a novel multifunctional BAC transgenic mouse reporter. *Dev Biol* 271:388–402.
19. Rieke F, Lee A, Haeseleer F (2008) Characterization of Ca2+-binding protein 5 knockout mouse retina. *Invest Ophthalmol Vis Sci* 49:5126–5135.
20. Haverkamp S, Haeseleer F, Hendrickson A (2003) A comparison of immunocytochemical markers to identify bipolar cell types in human and monkey retina. *Vis Neurosci* 20:589–600.
21. Dhingra A, et al. (2008) Probing neurochemical structure and function of retinal ON bipolar cells with a transgenic mouse. *J Comp Neurol* 510:484–496.
22. Koulen P, Fletcher EL, Craven SE, Bredt DS, Wässle H (1998) Immunocytochemical localization of the postsynaptic density protein PSD-95 in the mammalian retina. *J Neurosci* 18:10136–10149.
23. Kerekes RA, et al. (2011) Automated tracing of horizontal neuron processes during retinal development. *Neurochem Res* 36:583–593.
24. Peichl L, Gonzalez-Soriano J (1993)) Unexpected presence of neurofilaments in axon-bearing horizontal cells of the mammalian retina. *J Neurosci* 13(9):4091–4100.
25. Peichl L, González-Soriano J (1994) Morphological types of horizontal cell in rodent retinae: A comparison of rat, mouse, gerbil, and guinea pig. *Vis Neurosci* 11:501–517.
26. Zhang J, et al. (2004) Rb regulates proliferation and rod photoreceptor development in the mouse retina. *Nat Genet* 36:351–360.
27. Chattopadhyaya B, et al. (2004) Experience and activity-dependent maturation of perisomatic GABAergic innervation in primary visual cortex during a postnatal critical period. *J Neurosci* 24:9598–9611.